

Simulation Study for Engine Friction Reduction through the Enhancement of Temperature Distribution along Cylinder Liner in a Heavy Duty Diesel Engine

대형 상용 디젤 엔진의 실린더 라이너 온도 분포 개선을 통한 엔진 마찰 저감 - 해석적 연구

S. Y. Park*†

박 수 열*†

(received 14 October 2012, revised 19 October 2012, accepted 23 October 2012)

Key Words : 마찰 (Friction), 윤활(Lubrication), 실린더 라이너(Cylinder Liner), 열저항 코팅(Thermal Barrier Coating), 시뮬레이션(Simulation)

Abstract : 대형 상용 엔진에서 발생하는 유효 도시 마력의 약 4~15% 는 마찰 손실을 통해서 사라지며 마찰 손실 중 약 40~55%는 엔진 실린더와 피스톤 사이의 마찰에 의하여 발생하여, 엔진 전체에서 발생하는 마찰 손실 중 가장 많은 부분을 차지하고 있다. 이 연구에서는 엔진 실린더 라이너의 온도 분포 개선을 통해 라이너를 따라 유막을 형성하고 있는 윤활유의 적정 점성을 유지시키는 방법을 제시하고자 한다. 피스톤-라이너에서 발생하는 마찰 특성은 피스톤의 행정 위치에 따라서 접촉 마찰과 유막에 의한 마찰로 구분되며 이에 따라 요구되는 윤활유의 점성 특성 또한 달라진다. 먼저 해석 모델을 통하여 실린더 라이너 내부 온도 분포 특성을 확인한 후 피스톤 마찰 특성을 고려한 적정 온도 분포를 고찰하며 실린더 라이너에 열저항 코팅을 통해서 이를 구현하였다. 또한 실린더-피스톤 간의 마찰/윤활 해석을 통하여 열저항 코팅의 마찰 개선효과를 확인하였다.

1. 서 론

Vehicle fuel economy improvements are realized through a multitude of approaches, from engine downsizing, improved vehicle aerodynamics, electrification, waste heat recovery, and increased efficiency from existing vehicle systems. Fuel economy improvements in the engine can be realized through mechanical design, advanced control systems, material improvements, and friction reduction. Engine friction reduction is accomplished through three primary methods: mechanical design of engine components, material surface texture and coatings, and improvement in engine lubrication performance.¹⁾

About 10~15% of engine indicated mean effective pressure (IMEP) is lost by mechanical friction in a fired engine²⁾. The majority of the mechanical friction is attributed to the power cylinder assembly, which corresponds to 40~55% of the total friction²⁾ in a fired engine and piston ring and liner assembly is responsible for 28~45% of total power cylinder friction. This large contribution has made the power cylinder (specially, piston ring liner assembly) a primary focus in research and modeling efforts to better understand the tribological interfaces and physical phenomenon that occur. A schematic diagram for engine mechanical losses are summarized in Fig. 1.

*† 박수열(교신저자) : Postdoctoral Associate, Massachusetts Institute of Technology, Department of Mechanical Engineering
E-mail : sooyoul@mit.edu, Tel : 1-608-512-3595

† S. Y. Park(corresponding author) :Postdoctoral Associate, Massachusetts Institute of Technology, Department of Mechanical Engineering
E-mail : sooyoul@mit.edu, Tel : 1-608-512-3595

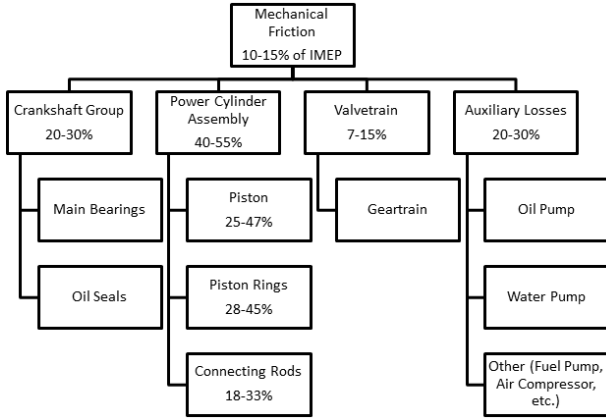


Fig. 1 schematic diagram of engine mechanical losses²⁾

A key parameter to determine the power cylinder friction is the viscosity of lubricant and it is highly dependent on temperature. Therefore, it is important to maintain optimal temperature along the power cylinder liner to minimize friction as well as to avoid engine wear by keeping appropriate viscosity along the cylinder liner. For this purpose, Thermal Barrier Coating (TBC) on the coolant side of the cylinder liner can be used to control the liner temperature as it is desired.

In this study, a concept for the optimal temperature distribution for the cylinder liner is introduced by analyzing the characteristics of the friction between cylinder liner and piston. The effect of TBC on the temperature distribution is investigated using heat conduction model. Then, its impact on the friction is studied by analyzing lubricant behavior between the liner and piston ring under different temperature distribution conditions.

2. Concept for reducing cylinder liner friction by controlling liner temperature

There are two kinds of friction regimes in piston moving; hydrodynamic friction and boundary friction. The hydrodynamic friction means that two moving parts separate each other by lubricant film and the friction is caused by viscosity of lubricant fluid. The boundary friction happens when two moving parts contact each other³⁾.

In the piston moving along a liner, hydrodynamic friction occurs during mid-stroke because piston speed is fast enough to develop thicker lubricant film than piston/liner roughness. On the other hand, the boundary friction is met near the Top Dead Center (TDC) and Bottom Dead Center (BDC) where the piston speed is low. The lubricant film thickness is smaller than the roughness of the piston/liner surface in this region. Moreover, TDC region is exposed to hot combustion gas longer than other regions of cylinder liner and lubricant becomes less viscous. Results for film thickness calculation and corresponding friction force will be shown and discussed in section 4.

From these features of piston-liner frictions, desirable viscosity and temperature distributions can be derived. Near TDC and BDC, high viscosity is required to avoid wear due to boundary friction because it is helpful to increase the film thickness and minimize probability of direct solid contact. Moving away from the TDC and BDC as piston speeds increase, the lubrication regime becomes hydrodynamic. In this regime, hydrodynamic drag and the high piston speeds at the mid-stroke lead to high friction. Ideally, hydrodynamic friction would be minimized in this region by reducing hydrodynamic drag inside the lubricant film. Lowering lubricant viscosity will generate lower hydrodynamic drag in the piston mid-stroke and lower frictional losses.

As discussed above, desirable lubricant viscosity are different between TDC/BDC and mid-stroke and one achievable way is to control the liner temperature. Viscosity of lubricant and temperature is highly correlated and Vogel equation as shown in equation (1) is usually used for this correlation. The parameters k , θ_1 , and θ_2 are constants determined for each lubricant with units of cSt for k and °C for θ_1 and θ_2 . T is the temperature of the lubricant in °C, and ν is the kinematic viscosity at the desired temperature in cSt.

$$\nu = k \exp\left(\frac{\theta_1}{\theta_2 + T}\right) \quad (1)$$

The cylinder liner of a heavy duty diesel engine is a separate component that is installed into the engine block using special gaskets. This configuration is called a wet liner because the outer walls of the cylinder liner are in direct contact with the engine coolant. The TBC is made on the coolant side of the liner. A schematic diagram for TBC is illustrated in Fig. 2.

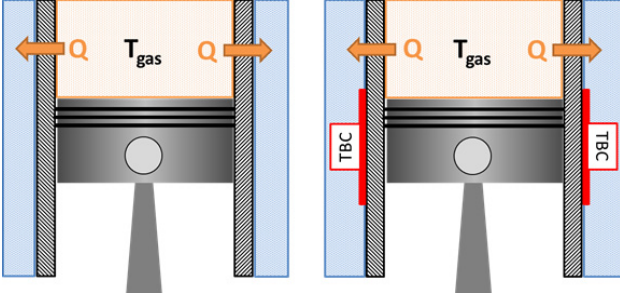


Fig. 2 Conventionally cooled cylinder liner and liner with Thermal Barrier Coating (TBC) on mid-stroke

Desirable material characteristics of a TBC for use in a diesel engine are low thermal conductivity and specific heat to provide insulating qualities. To survive in the engine a TBC must have high flexure strength, fracture toughness, and wear resistance to withstand the loads imposed on the TBC over time; thermal shock resistance to withstand the thermal cycles from engine on-off time; and chemical inertness.

Also critical is that the TBC have a coefficient of thermal expansion that is approximately the same as the metallic substrate it is to be applied on iron, steel, and aluminum.

Ytria Partially Stabilized Zirconia (YSZ) has been one of the most commonly used coating for diesel engines in recent studies. YSZ has proven performance in the coating of turbine blades that operate at temperatures around 1100 °C in thickness on the order of 100µm. YSZ is applied to metallic surfaces such as the cylinder liner using a thin metallic bond coat and then the insulating ceramic topcoat. The thermal conductivity of 8% YSZ is around 1.3W/m-K from 100 to 1200°C which is used in this study⁴⁾.

3. Simulation model

3.1 Prediction of cylinder liner temperature

In order to calculate the piston liner temperature, temperature of combustion gas should be calculated first and the First Law of Thermodynamics is used as presented in equation (2).

$$\left(1 + \frac{C_v}{R}\right)p \frac{dV}{d\theta} + \left(\frac{C_v}{R}\right)V \frac{dp}{d\theta} = \frac{dQ_{ch}}{d\theta} - \frac{dQ_{ht}}{d\theta} \quad (2)$$

where

p is the cylinder pressure

V is the cylinder volume

θ is the crank angle

C_v is the specific heat at constant volume

R is the gas constant

Q_{ch} is the chemical heat release from fuel combustion

Q_{ht} is the heat transfer to the surroundings

With equation (2), ideal gas law gives the gas temperature inside the engine cylinder. The combustion rate in the right hand side of equation (2) can be calculated by using simple Wiebe function which is presented in equation (3). The a_b , θ_s , θ_d and n are input parameters which determines the shape of Wiebe curve.

$$x_b(\theta) = 1 - \exp\left[-a_b \left(\frac{\theta - \theta_s}{\theta_d}\right)^n\right] \quad (3)$$

Charged mass of air in a cylinder is also required for equation (2) and equation (4) is used, which represents flow rate across a valve using compressible flow analysis. Important parameters are the upstream stagnation pressure, P_0 , and temperature, T_0 , and the static pressure immediately following the flow restriction, P_T . R is the gas constant, γ is the specific heat ratio, which is an input parameter in the model⁵⁾. C_D and A_R represent discharge coefficient and valve opening area respectively.

$$\dot{m} = \frac{C_D A_R P_0}{(R T_0)^{1/2}} \left(\frac{P_T}{P_0}\right)^{1/\gamma} \left\{ \left(\frac{2\gamma}{\gamma-1}\right) \left[1 - \left(\frac{P_T}{P_0}\right)^{(\gamma-1)/\gamma}\right] \right\}^{1/2} \quad (4)$$

The second term in the right hand side of equation (2) represents the heat transfer rate from engine cylinder to liner and it can be modeled using equation (5). The heat transfer coefficient, h_t can be found from simple Re–Nu correlation as shown in equation (6).

$$\frac{dQ_{ht}}{d\theta} = \frac{h_t A_t}{\omega} (T_g - T_L) \quad (5)$$

$$Nu = a Re^{0.7} \quad (6)$$

In equation (5) and (6), Re represents Reynolds number of combustion gas and Nu is Nusselt number. Heat transfer area, A_t is determined according to piston position. ω is engine rotational angular speed. T_g and T_L represent gas and liner temperature respectively.

The cylinder liner is discretized into 10 different segments which can have varying liner thicknesses, conductivities, TBC coating thickness, and TBC conductivity. Effects of conduction in the axial direction along the cylinder liner were included in the model to provide an accurate prediction of the axial liner temperature distribution. Coolant temperature is set to 375 K and a heat transfer coefficient is 5000 W/m²–K, based on values provided in literature⁽⁶⁾.

3.2 Cylinder liner lubrication

Cylinder liner friction is mainly caused by piston ring and piston skirt sliding. The piston skirt friction is mostly hydrodynamic friction because of relatively higher gap between piston skirt and liner than surface roughness. However, a friction regime for the piston ring pack is in both boundary and hydrodynamic friction regime. Hence, the piston ring friction is paid much attention to design the TBC coating strategy because of its transition of friction between boundary and hydrodynamic regime. In this study, only the piston ring friction model is employed for the study of TBC^(7–11).

One ring-pack model that has been used extensively in the automotive industry was developed at MIT by Tian, Wong, and Heywood⁽¹²⁾.

A diagram of the ring pack and liner interface is shown in Fig. 3. The piston ring pack model is based on Reynolds equation with the average flow factors as shown below in equation (7). U is the sliding velocity, h is the local fluid film thickness, μ is the lubricant viscosity, R_q is the roughness of the liner and ring surface, and Φ_p , Φ_g and Φ_s are flow factors that adjust the oil film pressure based on the surface characteristics. Once the equation (7) is solved, friction force by hydrodynamic drag can be found by equation (8).

$$\frac{\partial}{\partial x} \left(\Phi_p \frac{h^3}{\mu} \frac{\partial P}{\partial x} \right) = 6U \frac{\partial}{\partial x} (h\Phi_g + R_q\Phi_s) + 12 \frac{\partial h}{\partial t} \quad (7)$$

$$F_{hydrodynamic} = \int \left[\frac{\mu U}{h} (\Phi_g + \Phi_s) - \Phi_p \frac{h}{2} \frac{dP}{dx} \right] dA \quad (8)$$

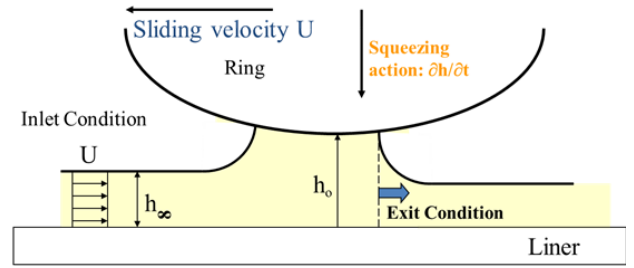


Fig. 3 Schematic diagram for piston ring-liner lubrication

When boundary friction occurs between the rings and liner, an analysis that is based on the Greenwood and Tripp^(13–14) asperity contact model is used as represented in equation (9).

Greenwood and Tripp's model describes the relationship of the elastic pressure of two contacting asperities with the distance between them. where σ is the combined asperity roughness of the two surfaces, (assumed to be equivalent to the combined surface roughness in this study), \mathcal{Q} is a limit beyond which contact is assumed to be negligible. N is the asperity density and β is the asperity radius of curvature. E' is average Young's modulus of two contact surfaces and A is correlation factor.

$$P_c\left(\frac{h}{\sigma}\right) = \frac{8\sqrt{2}}{15}\pi(N\beta'\sigma)E'A\left(\Omega - \frac{h}{\sigma}\right)^2 \text{ for } \frac{h}{\sigma} \leq \Omega \quad (9)$$

or

$$P_c\left(\frac{h}{\sigma}\right) = 0 \text{ for } \frac{h}{\sigma} > \Omega$$

4. Results and discussion

Simulations were run using a generic 5.9L diesel engine whose input parameters are outlined in Table 1. Since heat transfer between different cylinders in a multi-cylinder engine is not expected to vary significantly this simulation is run for a single cylinder only. A n engine operating point of 2500 RPM and a fueling rate of 45 kW was used for this generic simulation; which would correspond to approximately half load for an engine of this size.

With the baseline case established, applications of TBC from 0.5 to 3 mm thick were applied to the entire cylinder liner. The results for temperature distribution are shown in Fig. 4 and Fig. 5 for different coating configurations. Note that the x-axis represents each liner segment in the model with segment 1 occupying the top 1/10th of the liner length, and segment 10 corresponding to the bottom 1/10th of the liner length.

Table 1 Engine Dimensions

Engine Parameters	
Bore	102 mm
Stroke	120 mm
Connecting Rod Length	192 mm
Compression Ratio	17.5
Engine Speed	2500 Revolution Per Minute (RPM)

Results in Fig. 4 involves coating just the piston mid-stroke section of the liner, which corresponds to segments 4,5,6 in the model. As can be seen in Fig. 4, this causes the temperature in the mid-stroke region to raise approximately 35 to 60°C, depending on coating thickness. TDC region does not experience any significant increase in temperature. As noted previously, increasing TDC

temperature has significant effects on durability.

Fig. 5 displays the results for a liner TBC coating that extends from the beginning of the piston mid-stroke to BDC (segments 4–10). Similar to the results above, the TDC region does not experience any significant increase in temperature. The mid-stroke increases in temperature 35 to 60°C and at BDC the temperature increases 10 to 55°C depending on thermal barrier coating thickness.

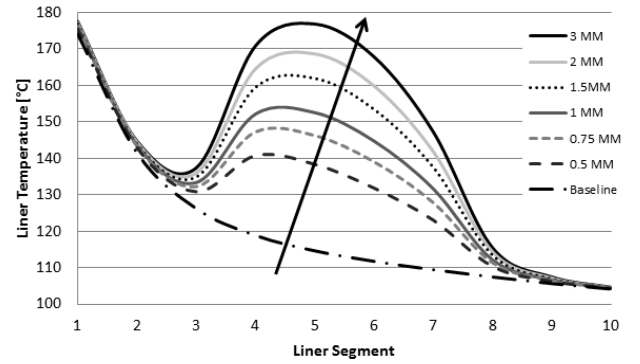


Fig. 4 Liner temperature with TBC on piston mid-stroke (segments 4,5,6)

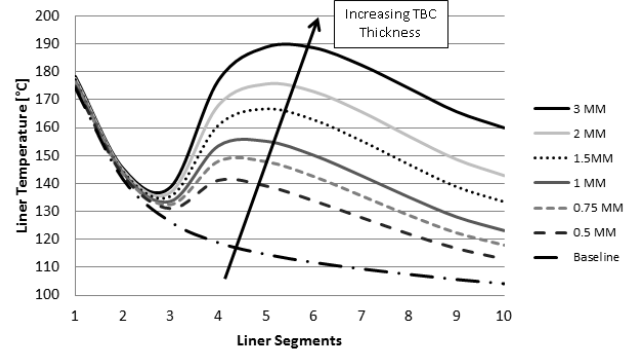


Fig. 5 Liner temperature with TBC on segments 4 through 10

Using the cylinder liner temperature profiles in Fig. 4 and 5, the Vogel equation was applied to generate the corresponding lubricant viscosity profile. The baseline lubricant selected for this part of the study was the 15W-40. Fig. 6 and Fig. 7 show the viscosity profiles along the cylinder liner for a liner coated in the mid-stroke, and a liner coated from mid-stroke to BDC, respectfully. Coating of the mid-stroke region produces actual

lubricant viscosity curves much closer to the desirable curve discussed in section 2. However, coating on mid-stroke to BDC gives decreases the viscosity from 12.5 cSt of baseline to 10 to 4 cSt depending on the coating thickness so it might cause the wear problem near BDC.

Using the viscosity profiles in Fig. 6 and 7, lubrication characteristics and friction force are calculated and results are presented in Fig. 8 to Fig. 10. For TBC cases, the 2 mm mid-stroke (segment 4,5,6) coating was chosen to compare with baseline case. Coating on segment 4 through 10 decreases the viscosity too much near BDC so it is not an desirable option.

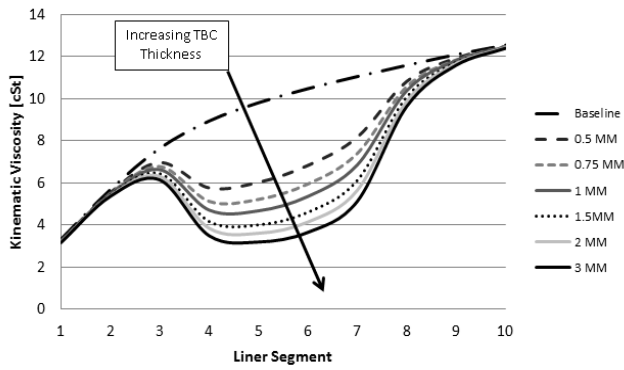


Fig. 6 Local viscosity of 15W-40 with TBC on liner segments 4,5,6

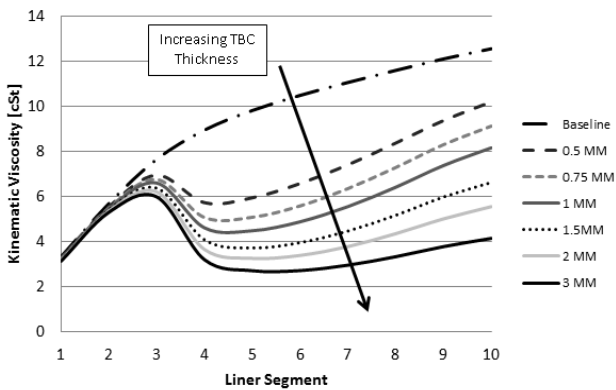


Fig. 7 Local viscosity of 15W-40 with TBC on liner segments 4 through 10

Fig. 8 shows variation of lubricant film thickness with respect to crank angle for baseline and TBC case. TBC decreases the lubricant film thickness significantly. Near the firing TDC, the film

thickness is less than $1 \mu\text{m}$ for both cases and friction is definitely in the boundary friction regime.

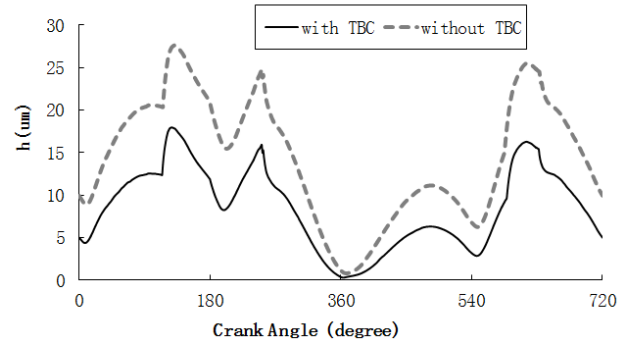


Fig. 8 Comparison of lubricant film thickness between baseline and TBC case of 2 mm thick and mid-stroke coating

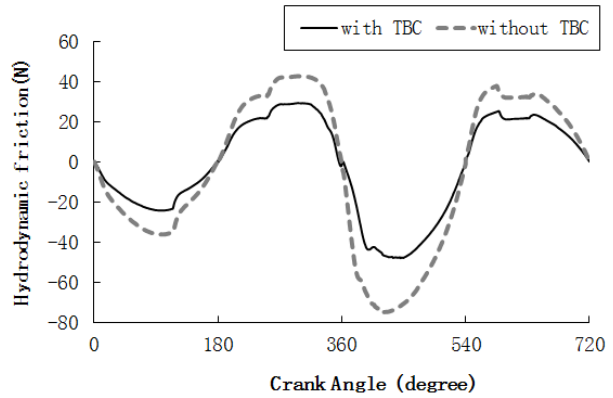


Fig. 9 Comparison of hydrodynamic friction between baseline and TBC case of 2 mm thick and mid-stroke coating

Then, hydrodynamic and boundary friction forces are compared between baseline and TBC case and results are presented in Fig. 9 and 10 respectively. From Fig. 9, it can be noticed that friction force decreases almost 40% over entire stroke. The negative sign means that piston movement changes its direction so only a magnitude of value is important. For example, at 90 degrees of crank angle, baseline (without TBC) case shows the friction force is -37N but it is almost -20N for TBC case.

Fig. 10 shows the comparison of boundary friction. The boundary friction increases a little for TBC case. However, its impact is only limited to

near TDC region, so it has little impact on entire friction force.

The total friction is sum of hydrodynamic friction and boundary friction and the total friction can be integrated over engine stroke to give Friction Mean Effective Pressure (FMEP).

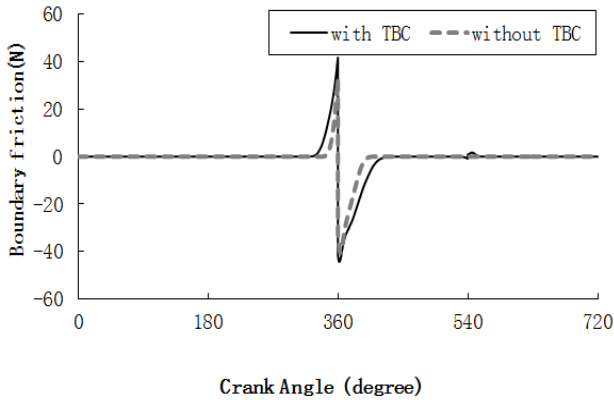


Fig. 10 Comparison of boundary friction between baseline and TBC case of 2 mm thick and mid-stroke coating

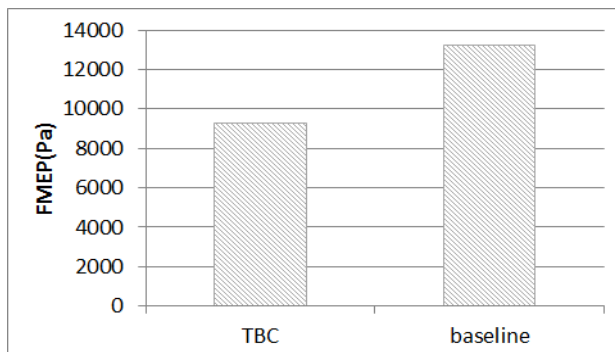


Fig. 11 Comparison of FMEP caused from piston ring and liner assembly between baseline and TBC case

Fig. 11 shows the comparison of FMEP for the piston ring–liner assembly between baseline and TBC case. FMEP decreases from 13300 Pa to 9300 Pa almost by 30%. This 30% of piston ring friction reduction can be translated into 0.6% of fuel economy enhancement using the engine friction information in Fig. 1.

5. Conclusions

In this research, the use of thermal barrier

coatings was investigated as a novel approach to strategically change cylinder liner temperatures in order to improve the power cylinder frictional losses. Simulation models were developed to calculate the cylinder liner temperature and lubrication/friction on the interface of piston ring and cylinder liner.

By coating selected parts of the liner where piston speeds are high, the local liner temperature is raised. In this region, the lubrication regime of the piston and liner interface is hydrodynamic and is where the majority of the power cylinder work losses occur due to the high surface speeds. By coating the liner strategically, top dead center temperatures are mostly unaffected. This is important because increasing liner temperature at TDC further decreases the oil film thickness, increasing boundary friction and wear. This approach is expected to maximize friction reduction while minimizing risk to other engine components or directionally increasing component wear rates.

Initial results have shown potential to decrease the piston skirt, piston ring, and cylinder liner interface friction around 30%. This corresponds to approximately a 0.5% to 1% improvement in vehicle fuel economy based on the engine friction information available in literatures.

Reference

1. R. Takata, Y. Li and V. Wong, 2006, "Effect of Liner Surface Texturing on Ring/Liner Friction in Large-Bore IC Engines," in Proceedings of ICEF06 ASME Internal Combustion Engine Division Fall Technical Conference, Sacramento, CA
2. D. Richardson, 2000, "Review of Power Cylinder Friction for Diesel Engines," Journal of Engineering for Gas Turbines and Power-Transactions of the ASME, vol. 122, no. 4, pp. 506–519
3. R. Takata, 2006, "Effects of Lubricant Viscosity and Surface Texturing on Ring-pack Performance in Internal Combustion Engines,"

MIT MS Thesis

4. G. Quian, T. Nakamura and C. Berndt, 1998, "The Effect of Thermal Gradient and Residual Stresses on Thermal Barrier Coating Fracture," *Mechanics of Materials*, vol. 27, pp. 91-110
5. J. Heywood, 1998, "Internal Combustion Engine Fundamentals", McGraw-Hill, New York, pp. 906-910
6. F. Shabir, S. Authars, S. Ganesan, R. Karthik and S. Madhan, 2010, "Low Heat Rejection Engines - Review," *SAE International Paper No. 2010-01-1510*
7. J. Booker, 1965, "Dynamically Loaded journal Bearings: Mobility Method of Solution," *ASME Journal of Basic Engineering*, pp. 537-546
8. K. Hamai, T. Masuda, T. Goto and S. Kai, 1990, "Development of a Friction Model for High Performance Engines," *Journal of the Society of Tribologists and Lubrication Engineers*, vol. 47, no. 7, pp. 567-573
9. G. Livanos and N. Kyrtatos, 2006, "A Model of the Friction Losses in Diesel Engines," in *SAE World Congress*, Detroit, Michigan, *SAE Paper No. 2006-01-0888*
10. G. Livanos, 2011, "Development of a Simplified Instantaneous Friction Model of the Piston-Crank-Slider Mechanism of Internal Combustion Engines," *SAE Paper No. 2011-01-0612*
11. E. Ciulli, 1992, "A Review of Internal Combustion Engine Losses Part 1: Specific Studies on the Motion of Pistons, Valves, and Bearings," *Proceedings of the Institution of Mechanical Engineers, Part D: Journal of Automobile Engineering*, vol. 206, no. 4, pp. 223-23
12. T. Tian, V. Wong and J. Heywood, 1996, "A Piston Ring Pack Film Thickness and Friction Model for Multigrade Oils and Rough Surfaces," in *SAE International Fall Fuels & Lubricants Meeting & Exposition*, *SAE Paper No. 962032*, San Antonio, Texas
13. N. Patir and H. Cheng, 1979, "Application of Average Flow Model to Lubrication Between Rough Sliding Surfaces," *ASME Journal of Lubrication Technology*
14. J. Greenwood and J. Tripp, 1971, "The Contact of Two Nominally Flat Surfaces," *Proceeding of the Institute of Mechanical Engineering*, vol. 185, pp. 625-633